Published in IET Radar, Sonar and Navigation
Received on 16th July 2013
Revised on 13th December 2013
Accepted on 13th December 2013
doi: 10.1049/iet-rsn.2013.0233

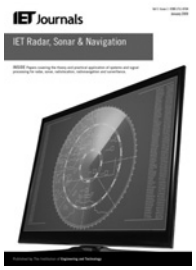

ISSN 1751-8784

Exploiting multiple a priori spectral models for adaptive radar detection

Augusto Aubry[1], Vincenzo Carotenuto[2], Antonio De Maio[2], Goffredo Foglia[3]

[1]*CNR, IREA, Via Diocleziano 328, Napoli I-80124, Italy*
[2]*Dipartimento di Ingegneria Elettrica e delle Tecnologie dell'Informazione, Universitá degli Studi di Napoli 'Federico II', Via Claudio 21, Napoli I-80125, Italy*
[3]*Elettronica S.p.A., Via Tiburtina km. 13.7, Roma I-00131, Italy*
E-mail: ademaio@unina.it

Abstract: This study deals with the problem of adaptive radar detection when a limited number of training data, due to environmental heterogeneity, is present. Suppose that some a priori spectral models for the interference in the cell under test and a lower bound on the power spectral density (PSD) of the white disturbance term are available. Hence, generalised likelihood ratio test-based detection algorithms have been devised. At the design stage, the basic idea is to model the actual interference inverse covariance as a combination of the available a priori models and to account for the available lower bound on the PSD. At the analysis stage, the capabilities of the new techniques have been shown to detect targets when few training data are available as well as their superiority with respect to conventional adaptive techniques based on the sample covariance matrix.

1 Introduction

Conventional adaptive radar receivers [1–3] require an estimate of the interference covariance matrix, performed through the training (secondary) data sample covariance. The training set is often composed of data vectors from range gates spatially close to the one under test and sharing the same spectral properties. This represents an important limitation since in real environments the number of data where the interference is homogeneous (often referred to as sample support) is very limited. Poor training data selection, in adaptive detectors, can lead to a remarkable degradation of radar performance especially in regions which include varying ground surfaces [4, 5]. A possible strategy to circumvent the lack of a sufficient number of homogeneous secondary data (required to achieve a satisfactory performance) is to exploit some a priori information about the scene illuminated by the radar, namely to perform a cognitive knowledge-based processing [6, 7, and references therein]. Alternatively, some structural information on the disturbance covariance matrix [8, 9] can be used for the estimation process.

In this paper, we devise adaptive detectors that jointly exploit some a priori knowledge available about the operating environment and training data (even if in a limited number) in order to confer robust adaptivity to the detectors. Otherwise stated, the idea is to exploit multiple spectral a priori models for the covariance matrix of the disturbance and suitably combine them (also accounting for the available information on a lower bound on the power spectral density (PSD) of the white disturbance term [10, 11]) in order to obtain an accurate estimate of the actual disturbance covariance. The training data rule the coefficients of the model combination. According to this guideline, exploiting the maximum likelihood (ML) principle, we propose some constrained estimates of the unknown parameters (target response and covariance matrix) compliant with the conditions that:

- the inverse covariance matrix of the interference plus noise is a combination of the a priori spectral models available for the operating environment;
- the estimated PSD of the white disturbance term is greater than or equal to the a priori known lower bound.

Hence, we exploit these estimates to devise three generalised likelihood ratio test (GLRT)-based detectors for the hypothesis testing problem under consideration. Two adaptive detectors are obtained resorting to the one-step GLRT design procedure, whereas the third relies on the two-step GLRT approach. Specifically, the former one-step GLRT is devised exploiting an iterative procedure to evaluate the constrained ML estimates of the unknown parameters and involves the solution of MAXDET convex optimisation problems [12, 13], which can be efficiently handled using interior point methods with a worst-case polynomial computational complexity. The latter one-step GLRT exploits heuristic estimates of the unknown parameters, and is characterised by a quite low computational complexity. Finally, the two-step GLRT is synthesised substituting the constrained ML estimate of the covariance matrix obtained from secondary data, into the

GLRT derived from the primary data assuming that the covariance matrix is known. This procedure leads to an adaptive matched filter (AMF)-like receiver where the conventional secondary data sample covariance matrix is replaced by the new constrained ML covariance estimate.

At the analysis stage, we assess the capabilities of the new covariance matrix estimators to track the actual clutter PSD (even with a very small number of secondary data) and show the superiority, in terms of detection probability, of the devised decision rules with respect to some conventional approaches based on the sample covariance matrix. Precisely, the analysis is conducted in comparison with the optimum detector, which assumes perfect knowledge of the interference covariance matrix, Kelly's GLRT [2] and AMF [3]. The detection probability results highlight that the proposed algorithms exhibit an acceptable performance loss with respect to the benchmark and can achieve interesting performance gains over Kelly's GLRT and AMF.

The paper is organised as follows: In Section 2, we formulate the problem and introduce the target and disturbance (interference plus noise) models. In Section 3, we devise the constrained estimates of the unknown parameters and design three adaptive detectors. In Section 4, we assess the performances of the proposed detectors and analyse the capability of the proposed covariance estimator to predict the actual interference environment. Finally, in Section 5, we draw conclusions and outline some possible future research tracks.

1.1 Notation

We adopt the notation of using boldface for vectors $\boldsymbol{a}$ (lower case), and matrices $\boldsymbol{A}$ (upper case). The conjugate transpose operator is denoted by the symbol $(\cdot)^{\dagger}$. tr$(\cdot)$ and det$(\cdot)$ are, respectively, the trace and the determinant of the square matrix argument. $\boldsymbol{I}$ and $\boldsymbol{0}$ denote, respectively, the identity matrix and the matrix with zero entries (their size is determined from the context). $\mathbb{C}^N$ and $\mathbb{H}^N$ are, respectively, the sets of N-dimensional vectors of complex numbers and of $N \times N$ Hermitian matrices. The Euclidean norm of the vector $\boldsymbol{x}$ is denoted by $\|\boldsymbol{x}\|$. $\lambda_{\max}(\boldsymbol{X})$ and $\lambda_{\min}(\boldsymbol{X})$ indicate the maximum and the minimum eigenvalue of $\boldsymbol{X} \in \mathbb{H}^N$, respectively. The curled inequality symbol $\succeq$ (and its strict form $\succ$) is used to denote generalised matrix inequality: For any $\boldsymbol{A} \in \mathbb{H}^N$, $\boldsymbol{A} \succeq \boldsymbol{0}$ means that $\boldsymbol{A}$ is a positive semi-definite matrix ($\boldsymbol{A} \succ \boldsymbol{0}$ for positive definiteness). The letter j represents the imaginary unit (i.e. $j = \sqrt{-1}$). For any complex number x, we use $\Re(x)$ and $\Im(x)$ to denote, respectively, the real and the imaginary part of x. Finally, $\mathbb{E}[\,\cdot\,]$ denotes statistical expectation.

2 Problem formulation and detectors design

We consider a monostatic radar that transmits a coherent train of N pulses and denote by $\boldsymbol{r} \in \mathbb{C}^N$ the N-dimensional vector of the samples obtained after base-band conversion, filtering and sampling at the range of interest the incoming waveform (primary data). We suppose the availability of secondary data $\boldsymbol{r}_i \in \mathbb{C}^N$, $i = 1, \ldots, K$, ($K \geq 0$), which do not contain useful target signal and exhibit the same covariance matrix as the primary data. Notice that, from a practical point of view, a data selection scheme [14, 15] can be employed for screening the available training data so as to excise possible outliers. Precisely, we focus on the following binary hypothesis testing problem

$$\begin{cases} H_0: \begin{cases} \boldsymbol{r} = \boldsymbol{n} \\ \boldsymbol{r}_i = \boldsymbol{n}_i, \quad i = 1, \ldots, K \end{cases} \\ H_1: \begin{cases} \boldsymbol{r} = \boldsymbol{n} + \alpha \boldsymbol{p} \\ \boldsymbol{r}_i = \boldsymbol{n}_i, \quad i = 1, \ldots, K \end{cases} \end{cases} \tag{1}$$

where $\boldsymbol{p} \in \mathbb{C}^N$ denotes the unitary norm steering vector of the target and $\alpha \in \mathbb{C}$ is an unknown parameter accounting for both target reflectivity and channel propagation effects. As to the interference plus noise random vectors, we model $\boldsymbol{n}$ and $\boldsymbol{n}_i$s, $i = 1, \ldots, K$, as independent, complex, zero-mean, circular symmetric Gaussian vectors sharing the same covariance matrix $\boldsymbol{M} \succ \boldsymbol{0}$, namely

$$\mathbb{E}[\boldsymbol{n}\boldsymbol{n}^{\dagger}] = \mathbb{E}\left[\boldsymbol{n}_i \boldsymbol{n}_i^{\dagger}\right] = \boldsymbol{M}, \quad i = 1, \ldots, K$$

Subsequent developments require specifying the complex multivariate probability density function (pdf) of the observable matrix $\boldsymbol{R} = [\boldsymbol{r}, \boldsymbol{r}_1, \ldots, \boldsymbol{r}_K]$ under both the hypotheses. Denoting by $\boldsymbol{X} = \boldsymbol{M}^{-1}$, the inverse disturbance covariance matrix, previous assumptions imply that

$$f_{\boldsymbol{R}}(\boldsymbol{R}|\boldsymbol{X}, H_0) = \frac{\det(\boldsymbol{X})^{(K+1)}}{\pi^{N(K+1)}} \exp\left(-\mathrm{tr}\left\{\boldsymbol{X}\boldsymbol{R}\boldsymbol{R}^{\dagger}\right\}\right) \tag{2}$$

and

$$f_{\boldsymbol{R}}(\boldsymbol{R}|\boldsymbol{X}, \alpha, H_1) = \frac{\det(\boldsymbol{X})^{(K+1)}}{\pi^{N(K+1)}} \exp\left(-\mathrm{tr}\left\{\boldsymbol{X}\left(\boldsymbol{R}_{\alpha} + K\boldsymbol{S}\right)\right\}\right) \tag{3}$$

with $\boldsymbol{S} = (1/K)\sum_{i=1}^{K} \boldsymbol{r}_i \boldsymbol{r}_i^{\dagger}$, the sample covariance matrix of the secondary data, and $\boldsymbol{R}_{\alpha} = (\boldsymbol{r} - \alpha \boldsymbol{p})(\boldsymbol{r} - \alpha \boldsymbol{p})^{\dagger}$.

According to the Neyman–Pearson criterion, the optimum solution to the hypothesis testing problem (1) is the likelihood ratio test (LRT). However, for the case under consideration, this procedure does not lead to a uniformly most powerful test as the resulting detector requires the knowledge of the parameters α and $\boldsymbol{X}$, which reasonably are assumed to be unknown. A possible way to cope with the aforementioned a priori uncertainty is to resort to adaptive detectors, where the unknown parameters appearing in nominal decision statistics are replaced by suitable estimates.

Conventional adaptive algorithms, such as Kelly's GLRT and AMF, assume at the design stage a homogeneous training set whose cardinality K is greater than or equal to N and exploit the sample covariance matrix computed from the secondary data. Additionally, to achieve a good detection performance, K has to be greater than or equal to $2N$. Unfortunately, in practical radar scenarios, such assumption is not always valid [16]. More specifically, the size of the training set is often limited, namely, the large swaths of homogeneous clutter/interference necessary for accurately estimating $\boldsymbol{M}$ through the sample covariance matrix may not be available. Finally, the analysis of several adaptive algorithms, mostly designed assuming homogeneity of the secondary data, has shown that non-homogeneities magnify the loss between the adaptive implementation and optimum conditions [4, 5].

The idea followed in this paper is to exploit some a priori information about the interfering environment so as to suitably describe, and hence constrain, the interference plus noise covariance matrix. By doing so, the sample support

doi: 10.1049/iet-rsn.2013.0233

requirement is reduced while keeping good detection performance. Precisely, it is assumed:

- the availability of multiple a priori models for the interference PSD. Each of them corresponds to a model for the inverse interference covariance matrix $\boldsymbol{X}$; these inverse covariance models, $\boldsymbol{X}_i$, $i=0,\ \ldots,\ H$, are assumed positive-definite, that is, $\boldsymbol{X}_i \succ \boldsymbol{0}, \quad i=0,\ \ldots,\ H$;
- the availability of a lower bound σ^2 on the PSD level of the white disturbance term σ_0^2, that is, $\sigma_0^2 \geq \sigma^2$.

Otherwise stated, it is supposed that $\boldsymbol{X}$ belongs to the uncertainty set

$$\mathcal{A} = \left\{ \boldsymbol{X}' \succ \boldsymbol{0} : \boldsymbol{X}' = \sum_{i=0}^{H} t_i \boldsymbol{X}_i, \ \boldsymbol{X}' \preceq \frac{\boldsymbol{I}}{\sigma^2}, \quad t_i \in \mathbb{R}, \quad i=0,\ \ldots,\ H \right\} \tag{4}$$

The following section proposes some constrained estimates of the unknown parameters α and $\boldsymbol{X}$ based on the ML principle. These estimates are exploited to devise some adaptive detectors for the hypothesis testing problem (1).

3 Estimates of the unknown parameters and adaptive detectors

A possible strategy to estimate the unknown parameters α and $\boldsymbol{X}$ accounting for the covariance structure (4), is to resort to the constrained ML approach. Specifically, the constrained ML estimates of the unknown parameters under the hypotheses H_0 and H_1 are optimal solutions, respectively, to the optimisation problems $\mathcal{P}_{H_0}$ and $\mathcal{P}_{H_1}$, defined in (5)

where $\Theta_{H_0} = \{0\}$ and $\Theta_{H_1} = \mathbb{C}$. To obtain the sought estimates, let us define the following MAXDET convex optimisation problem [12], parameterised in the positive semi-definite matrix $\boldsymbol{S}_1 \succeq 0$

$$\mathcal{P}(\boldsymbol{S}_1) \begin{cases} \min\limits_{\boldsymbol{X}} & \operatorname{tr}(\boldsymbol{S}_1 \boldsymbol{X}) - \log \quad \det(\boldsymbol{X}) \\ \text{subject to} & \boldsymbol{X} \in \mathcal{A} \end{cases} \tag{6}$$

Recalling that by 'solvable', we mean that the problem is feasible and bounded below, and the optimal value is attained, see [17, p. 13] the following proposition summarises the key properties of problem $\mathcal{P}(\boldsymbol{S}_1)$.

Proposition 1: For any $\boldsymbol{S}_1 \succeq \boldsymbol{0}$, problem $\mathcal{P}(\boldsymbol{S}_1)$ is solvable and admits a unique optimal solution. Additionally, its optimal solution can be efficiently computed in polynomial time using interior point methods.

Proof: See Appendix 1.

Algorithm 1

Input: $\boldsymbol{S}$, $\boldsymbol{r}$ and K.
Output: $\hat{\boldsymbol{X}}_{H_0}$.

1: Estimate the covariance matrix under H_0:
- Let $\boldsymbol{S}_1 = \frac{1}{K+1}\left(K\boldsymbol{S} + \boldsymbol{r}\boldsymbol{r}^{\dagger}\right)$;
- Compute $\hat{t}_i = \min\left(\frac{1}{\sigma^2 \lambda_{max}(\boldsymbol{X}_i)}, \frac{N}{\operatorname{tr}(\boldsymbol{S}_1 \boldsymbol{X}_i)}\right), \ i=0,\ldots,H;$
- Evaluate $\hat{\boldsymbol{X}}_{H_0} = \frac{1}{H+1}\sum_{i=0}^{H} \hat{t}_i \boldsymbol{X}_i$.

2: Return $\hat{\boldsymbol{X}}_{H_0}$.

Fig. 1 *Algorithm 1*

Estimation algorithms under H_0: Resorting to Proposition 1, the ML estimate $\hat{\boldsymbol{X}}_{H_0}^{ML}$ of $\boldsymbol{X}$ under H_0 can be obtained solving $\mathcal{P}(\boldsymbol{S}_1)$ with $\boldsymbol{S}_1 = \frac{1}{(K+1)}(K\boldsymbol{S} + \boldsymbol{r}\boldsymbol{r}^{\dagger})$. Hence, the ML estimate can be computed in polynomial time.

Notice that, from a practical point of view, it is also of interest to introduce a simplified (even if sub-optimum) approach to minimising the objective function in $\mathcal{P}_{H_0}$. Towards this goal, we devise a heuristic estimate $\hat{\boldsymbol{X}}_{H_0}$ of $\boldsymbol{X}$ under H_0; the main guideline is to reduce as much as possible the computational complexity of the optimisation procedure while keeping good estimation performances. To this end, we first estimate the inverse covariance matrix assuming that only the model $\boldsymbol{X}_i$ is active, $i=0,\ \ldots,\ H$, then we compute the arithmetic mean of the resulting estimates. Precisely, for a specific model $\boldsymbol{X}_i$, $i=0,\ \ldots,\ H$, exploiting the concavity of the log-likelihood function, the ML estimate of $\boldsymbol{X}$, is given by

$$\hat{\boldsymbol{X}}_i = \min\left(\frac{1}{\sigma^2 \lambda_{\max}(\boldsymbol{X}_i)}, \frac{N}{\operatorname{tr}(\boldsymbol{S}_1 \boldsymbol{X}_i)}\right)\boldsymbol{X}_i, \quad i=0,\ \ldots,\ H$$

where $(N/\operatorname{tr}(\boldsymbol{S}_1\boldsymbol{X}_i))$ is obtained nulling the derivative of the log-likelihood function with respect to t_i, that is, solving the equation

$$\frac{\mathrm{d}}{\mathrm{d}t_i}\left[-\operatorname{tr}(\boldsymbol{S}_1 t_i \boldsymbol{X}_i) + \log\det(t_i \boldsymbol{X}_i)\right] = -\operatorname{tr}(\boldsymbol{S}_1 \boldsymbol{X}_i) + \frac{N}{t_i} = 0 \tag{7}$$

with $\boldsymbol{S}_1 = \frac{1}{(K+1)}(K\boldsymbol{S} + \boldsymbol{r}\boldsymbol{r}^{\dagger})$.

Algorithm 1, reported in Fig. 1, summarises the steps for the computation of the unknown covariance matrix, compliant with the model (4).

Estimation algorithms under H_1: Let us now focus on $\mathcal{P}_{H_1}$. To minimise the objective function and obtain suitable estimates $\hat{\alpha}^{\mathrm{ML}}$ and $\hat{\boldsymbol{X}}_{H_1}^{\mathrm{ML}}$ of α and $\boldsymbol{X}$, we propose an alternating optimisation procedure. The idea is to iteratively maximise the likelihood. Specifically, starting from a target response estimate $\hat{\alpha}^{(n-1)}$, we compute the ML inverse covariance estimate $\hat{\boldsymbol{X}}_{H_1}^{(n)}$, at step n compliant with model

$$\mathcal{P}_{H_k} \begin{cases} \min\limits_{\alpha, \boldsymbol{X}} & \operatorname{tr}\left\{\boldsymbol{X}\left[\frac{1}{K+1}\left(\boldsymbol{R}_{\alpha} + K\boldsymbol{S}\right)\right]\right\} - \log \quad \det(\boldsymbol{X}) \\ \text{subject to} & \boldsymbol{X} \in \mathcal{A} \\ & \alpha \in \Theta_{H_k} \end{cases} \qquad k=0,\ 1 \tag{5}$$

Algorithm 2

Input: $\boldsymbol{S}$, $\boldsymbol{r}$, $\boldsymbol{p}$, K and ζ.
Output: $\hat{\alpha}^{ML} = \hat{\alpha}^{(n)}$, $\hat{\boldsymbol{X}}_{H_1}^{ML} = \hat{\boldsymbol{X}}_{H_1}^{(n)}$ and $\widetilde{\mathrm{ML}}^{\star} = \widetilde{\mathrm{ML}}^{(n)}$.

1: set $n = 0$, $\alpha^{(n)} = \frac{\boldsymbol{p}^{\dagger}\boldsymbol{r}}{\|\boldsymbol{p}\|^2}$, $\boldsymbol{R}_{\hat{\alpha}^{(n)}} = (\boldsymbol{r} - \alpha^{(n)}\boldsymbol{p})(\boldsymbol{r} - \alpha^{(n)}\boldsymbol{p})^{\dagger}$, and $\mathrm{ML}^{(n)} = -\zeta$;
2: **do**
3: $n := n + 1$;
4: Estimate the inverse covariance matrix:
solve the MAXDET problem $\mathcal{P}(\boldsymbol{S}_1)$, with $\boldsymbol{S}_1 = \frac{1}{K+1}(K\boldsymbol{S} + \boldsymbol{R}_{\hat{\alpha}^{(n-1)}})$, finding the ML estimate $\hat{\boldsymbol{X}}_{H_1}^{(n)}$.
5: Estimate the target complex amplitude:

$$\hat{\alpha}^{(n)} = \frac{\boldsymbol{p}^{\dagger}\hat{\boldsymbol{X}}_{H_1}^{(n)}\boldsymbol{r}}{\boldsymbol{p}^{\dagger}\hat{\boldsymbol{X}}_{H_1}^{(n)}\boldsymbol{p}}.$$

6: compute $\boldsymbol{R}_{\hat{\alpha}^{(n)}}$ and

$$\widetilde{\mathrm{ML}}^{(n)} = \det(\hat{\boldsymbol{X}}_{H_1}^{(n)})^{K+1} \exp\left(-\mathrm{tr}\left\{\hat{\boldsymbol{X}}_{H_1}^{(n)}(\boldsymbol{R}_{\hat{\alpha}^{(n)}} + K\boldsymbol{S})\right\}\right)$$

7: **until** $|\widetilde{\mathrm{ML}}^{(n)} - \widetilde{\mathrm{ML}}^{(n-1)}| > \zeta$
8: Return $\hat{\alpha}^{ML} = \hat{\alpha}^{(n)}$, $\hat{\boldsymbol{X}}_{H_1}^{ML} = \hat{\boldsymbol{X}}_{H_1}^{(n)}$ and $\widetilde{\mathrm{ML}}^{\star} = \widetilde{\mathrm{ML}}^{(n)}$.

Fig. 2 *Algorithm 2*

(4). Whenever $\hat{\boldsymbol{X}}_{H_1}^{(n)}$ is found, we search for the ML target response $\hat{\alpha}^{(n)}$, and so on. Notice that, $\hat{\alpha}^{(n)}$ can be computed in closed form nulling the derivative of the log-likelihood function with respect to α, that is

$$\hat{\alpha}^{(n)} = \frac{\boldsymbol{p}^{\dagger}\hat{\boldsymbol{X}}_{H_1}^{(n)}\boldsymbol{r}}{\boldsymbol{p}^{\dagger}\hat{\boldsymbol{X}}_{H_1}^{(n)}\boldsymbol{p}}$$

As to $\hat{\boldsymbol{X}}_{H_1}^{(n)}$, it is given by the optimal solution to problem $\mathcal{P}(\boldsymbol{S}_1)$, with $\boldsymbol{S}_1 = \left[\frac{1}{K+1}\right](K\boldsymbol{S} + \boldsymbol{R}_{\hat{\alpha}^{(n-1)}})$.

Algorithm 2, represented in Fig. 2, describes the steps of the proposed sequential optimisation procedure.

The proposed optimisation technique shares some interesting properties summarised in the following proposition:

Proposition 2: Let $\left\{\left(\hat{\alpha}^{(n)}, \hat{\boldsymbol{X}}_{H_1}^{(n)}\right)\right\}$ be a sequence of points obtained through the proposed sequential optimisation procedure; let $\mathrm{ML}^{(n)}$ be the likelihood value corresponding to the point $\left\{\left(\hat{\alpha}^{(n)}, \hat{\boldsymbol{X}}_{H_1}^{(n)}\right)\right\}$ at the nth iteration. Then,

- the sequence $\mathrm{ML}^{(n)}$ is a monotonic increasing sequence;
- the sequence $\mathrm{ML}^{(n)}$ converges to a finite value $\mathrm{ML}^{\star}$.

Proof: See Appendix 2.

Let us now introduce two heuristic procedures, characterised by a low computational complexity, for estimating α and $\boldsymbol{X}$ under H_1. Both the techniques operate as follows:

1. estimate the inverse covariance matrix, $\hat{\boldsymbol{X}}$ say;
2. compute the ML estimate of α resulting from the computed estimate $\hat{\boldsymbol{X}}$, that is, $\hat{\alpha} = (\boldsymbol{p}^{\dagger}\hat{\boldsymbol{X}}\boldsymbol{r}/\boldsymbol{p}^{\dagger}\hat{\boldsymbol{X}}\boldsymbol{p})$.

However, they differ for the adopted inverse covariance matrix estimate. The first procedure extends Algorithm 1, to account for the presence of the useful signal in the primary data. Specifically, it first estimates the inverse covariance matrix assuming that only model $\boldsymbol{X}_i$ is active, $i = 0, \ldots, H$, then it computes the arithmetic mean of the quoted estimates. According to this guideline, when it is assumed that only the model ith is active, the ML estimate of $\boldsymbol{X}$ can be obtained in closed form as

$$\hat{\boldsymbol{X}}_i = \min\left(\frac{1}{\sigma^2\lambda_{\max}(\boldsymbol{X}_i)}, \frac{N}{\mathrm{tr}\left(\left(\frac{1}{K+1}\right)(\boldsymbol{R}_{\hat{\alpha}_i} + K\boldsymbol{S})\boldsymbol{X}_i\right)}\right)\boldsymbol{X}_i,$$
$$i = 0, \ldots, H \tag{8}$$

with $\hat{\alpha}_i = (\boldsymbol{p}^{\dagger}\hat{\boldsymbol{X}}_i\boldsymbol{r}/\boldsymbol{p}^{\dagger}\hat{\boldsymbol{X}}_i\boldsymbol{p})$, $i = 0, \ldots, H$.

The second proposed sub-optimum estimation procedure (this technique assumes $K \geq 1$) performs the constrained ML estimation of $\boldsymbol{X}$ only exploiting secondary data, which are assumed free of the useful target signal. Hence, the computed estimate is the optimal solution to the optimisation problem $\mathcal{P}(\boldsymbol{S}_1)$ with $\boldsymbol{S}_1 = \boldsymbol{S}$.

Algorithms 3 and 4, reported in Figs. 3 and 4, respectively, summarise the steps for the computation of the target

Algorithm 3

Input: $\boldsymbol{S}$, $\boldsymbol{r}$, $\boldsymbol{p}$ and K.
Output: $\hat{\alpha}_1$ and $\hat{\boldsymbol{X}}_{H_1,1}$.

1: Estimate the covariance matrix under H_1:
- Let $\hat{\alpha}_i = \frac{\boldsymbol{p}^{\dagger}\boldsymbol{X}_i\boldsymbol{r}}{\boldsymbol{p}^{\dagger}\boldsymbol{X}_i\boldsymbol{p}}$, $i = 0, \ldots, H$, and compute

$$\boldsymbol{R}_{\hat{\alpha}_i} = (\boldsymbol{r} - \hat{\alpha}_i\boldsymbol{p})(\boldsymbol{r} - \hat{\alpha}_i\boldsymbol{p})^{\dagger},\ i = 0, \ldots, H$$

$$\bar{\boldsymbol{S}}_i = \tfrac{1}{K+1}(\boldsymbol{R}_{\hat{\alpha}_i} + K\boldsymbol{S}),\ i = 0, \ldots, H$$

- Compute $\hat{t}_i = \min\left(\frac{1}{\sigma^2\lambda_{max}(\boldsymbol{X}_i)}, \frac{N}{\mathrm{tr}(\boldsymbol{X}_i\bar{\boldsymbol{S}}_i)}\right)$, $i = 0, \ldots, H$
- Evaluate the sample matrix $\hat{\boldsymbol{X}}_{H_1,1} = \frac{1}{H+1}\sum_{i=0}^{H}\hat{t}_i\boldsymbol{X}_i$

2: Estimate the target complex amplitude:

$$\hat{\alpha}_1 = \frac{\boldsymbol{p}^{\dagger}\hat{\boldsymbol{X}}_{H_1,1}\boldsymbol{r}}{\boldsymbol{p}^{\dagger}\hat{\boldsymbol{X}}_{H_1,1}\boldsymbol{p}}.$$

3: Return $\hat{\alpha}_1$ and $\hat{\boldsymbol{X}}_{H_1,1}$.

Fig. 3 *Algorithm 3*

doi: 10.1049/iet-rsn.2013.0233

Algorithm 4

Input: $\boldsymbol{S}$, $\boldsymbol{r}$, $\boldsymbol{p}$.
Output: $\hat{\alpha}_2$ and $\hat{\boldsymbol{X}}_{H_1,2}$.

1: Estimate the inverse covariance matrix:
solve the MAXDET problem $\mathcal{P}(\boldsymbol{S}_1)$, with $\boldsymbol{S}_1 = \boldsymbol{S}$ finding the estimate $\hat{\boldsymbol{X}}_{H_1,2}$
2: Estimate the target complex amplitude:

$$\hat{\alpha}_2 = \frac{\boldsymbol{p}^{\dagger}\hat{\boldsymbol{X}}_{H_1,2}\boldsymbol{r}}{\boldsymbol{p}^{\dagger}\hat{\boldsymbol{X}}_{H_1,2}\boldsymbol{p}}.$$

3: Return $\hat{\alpha}_2$ and $\hat{\boldsymbol{X}}_{H_1,2}$.

Fig. 4 *Algorithm 4*

response and unknown covariance matrix. In the following subsections, we devise some adaptive receivers exploiting the proposed estimates.

3.1 Adaptive detectors

In this subsection, we design some GLRT-based detectors exploiting the devised estimates of the unknown parameters α and $\boldsymbol{X}$. Precisely, we exploit both one-step and two-step GLRT-based design procedures to solve the hypothesis testing problem (1).

One-step GRLT-based detectors: Strictly speaking, the one-step GLRT criterion is tantamount to replacing the unknown parameters with their ML estimates under each hypothesis, namely it is the following decision rule

$$\frac{\max_{\alpha\in\mathbb{C},\boldsymbol{X}\in\mathcal{A}} \det(\boldsymbol{X})^{K+1}\exp\left(-\mathrm{tr}\left\{\boldsymbol{X}\left[\boldsymbol{R}_{\alpha}+K\boldsymbol{S}\right]\right\}\right)}{\max_{\boldsymbol{X}\in\mathcal{A}} \det(\boldsymbol{X})^{K+1}\exp\left(-\mathrm{tr}\left\{\boldsymbol{X}\left[\boldsymbol{r}\boldsymbol{r}^{\dagger}+K\boldsymbol{S}\right]\right\}\right)} \underset{H_0}{\overset{H_1}{\gtrless}} \eta \quad (9)$$

where η is the detection threshold. The proposed one-step GLRT-based detectors approximate (9) replacing the ML estimates involved in the numerator and denominator of (9) with the estimates developed in Section 3. Precisely, the synthesised decision rules are, respectively, given by

$$l_1 = \frac{\det\left(\hat{\boldsymbol{X}}_{H_1}^{\mathrm{ML}}\right)^{K+1}\exp\left(-\mathrm{tr}\left\{\hat{\boldsymbol{X}}_{H_1}^{\mathrm{ML}}\left[\boldsymbol{R}_{\hat{\alpha}^{\mathrm{ML}}}+K\boldsymbol{S}\right]\right\}\right)}{\det\left(\hat{\boldsymbol{X}}_{H_0}^{\mathrm{ML}}\right)^{K+1}\exp\left(-\mathrm{tr}\left\{\hat{\boldsymbol{X}}_{H_0}^{\mathrm{ML}}\left(\boldsymbol{r}\boldsymbol{r}^{\dagger}+K\boldsymbol{S}\right)\right\}\right)} \underset{H_0}{\overset{H_1}{\gtrless}} \eta_1 \quad (10)$$

where η_1 is the detection threshold, $\hat{\alpha}^{\mathrm{ML}}$ and $\hat{\boldsymbol{X}}_{H_1}^{\mathrm{ML}}$ are obtained through Algorithm 2, and $\hat{\boldsymbol{X}}_{H_0}^{\mathrm{ML}}$ is the optimal solution to $\mathcal{P}(\boldsymbol{S}_1)$ with $\boldsymbol{S}_1 = \frac{1}{(K+1)}(K\boldsymbol{S}+\boldsymbol{r}\boldsymbol{r}^{\dagger})$. This receiver will be referred to as GLRT-1 in the following:

$$l_2 = \frac{\det\left(\hat{\boldsymbol{X}}_{H_1,1}\right)^{K+1}\exp\left(-\mathrm{tr}\left\{\hat{\boldsymbol{X}}_{H_1,1}\left(\boldsymbol{R}_{\hat{\alpha}_1}+K\boldsymbol{S}\right)\right\}\right)}{\det\left(\hat{\boldsymbol{X}}_{H_0}\right)^{K+1}\exp\left(-\mathrm{tr}\left\{\hat{\boldsymbol{X}}_{H_0}\left(\boldsymbol{r}\boldsymbol{r}^{\dagger}+K\boldsymbol{S}\right)\right\}\right)} \underset{H_0}{\overset{H_1}{\gtrless}} \eta_2 \quad (11)$$

where η_2 is the detection threshold, $\hat{\alpha}_1$ and $\hat{\boldsymbol{X}}_{H_1,1}$ are obtained through Algorithm 3, and $\hat{\boldsymbol{X}}_{H_0}$ is the output to Algorithm 1. This receiver will be referred to as GLRT-2 in the following.

Two-step GRLT-based detector: The two-step GLRT criterion is tantamount to substituting a suitable estimate $\hat{\boldsymbol{X}}$ for the unknown inverse covariance matrix into the GLRT derived assuming that $\boldsymbol{X}$ is known. According to this guideline, given $\boldsymbol{X}$, the GLRT is

$$\frac{\max_{\alpha\in\mathbb{C}} \det(\boldsymbol{X})^{K+1}\exp\left(-\mathrm{tr}\left\{\boldsymbol{X}\left[\boldsymbol{R}_{\alpha}+K\boldsymbol{S}\right]\right\}\right)}{\det(\boldsymbol{X})^{K+1}\exp\left(-\mathrm{tr}\left\{\boldsymbol{X}\left[\boldsymbol{r}\boldsymbol{r}^{\dagger}+K\boldsymbol{S}\right]\right\}\right)} \underset{H_0}{\overset{H_1}{\gtrless}} \eta \quad (12)$$

where η is the detection threshold. Hence, the proposed two-step GLRT detector substitutes the constrained ML estimate of the disturbance covariance matrix based on the secondary data in place of $\boldsymbol{X}$ in (12), namely, it can be computed as

$$\begin{aligned} l_3 &= \frac{\left|\boldsymbol{p}^{\dagger}\hat{\boldsymbol{X}}_{H_1,2}\boldsymbol{r}\right|^2}{\boldsymbol{p}^{\dagger}\hat{\boldsymbol{X}}_{H_1,2}\boldsymbol{p}} \\ &= \log\left(\frac{\det(\boldsymbol{X}_{H_1,2})^{K+1}\exp\left(-\mathrm{tr}\left\{\hat{\boldsymbol{X}}_{H_1,2}\left(\boldsymbol{R}_{\hat{\alpha}_2}+K\boldsymbol{S}\right)\right\}\right)}{\det(\boldsymbol{X}_{H_1,2})^{K+1}\exp\left(-\mathrm{tr}\left\{\hat{\boldsymbol{X}}_{H_1,2}\left(\boldsymbol{r}\boldsymbol{r}^{\dagger}+K\boldsymbol{S}\right)\right\}\right)}\right) \underset{H_0}{\overset{H_1}{\gtrless}} \eta_3 \end{aligned} \quad (13)$$

where η_3 is the detection threshold, while $\hat{\alpha}_2$ and $\hat{\boldsymbol{X}}_{H_1,2}$ are obtained through Algorithm 4. This receiver will be referred to as GLRT-3 in the following. Interestingly, it can be interpreted as the AMF receiver [3] where the conventional sample covariance matrix $\boldsymbol{S}$, computed from the secondary data is replaced with the constrained ML estimate $\hat{\boldsymbol{X}}_{H_1,2}^{-1}$, accounting for the structural model (4).

An important remark concerning computational complexity is now in order.

- GLRT-1 exploits an iterative procedure (alternating optimisations) to maximise the numerator of (9). This implies the solution of as many MAXDET problems as the number of required iterations to satisfy condition 7 in Algorithm 1.
- GLRT-3 does not require iterative optimisations but exploits one-shot sub-optimum estimates of the unknown parameters. A single MAXDET problem has to be solved. Otherwise stated, GLRT-3 requires a computational effort smaller than GLRT-1.
- GLRT-2 does not require iterative optimisations but exploits one-shot sub-optimum estimates of the unknown parameters. Additionally, no MAXDET problem has to be solved. Otherwise stated, GLRT-2 requires a computational effort much smaller than both GLRT-1 and GLRT-3.

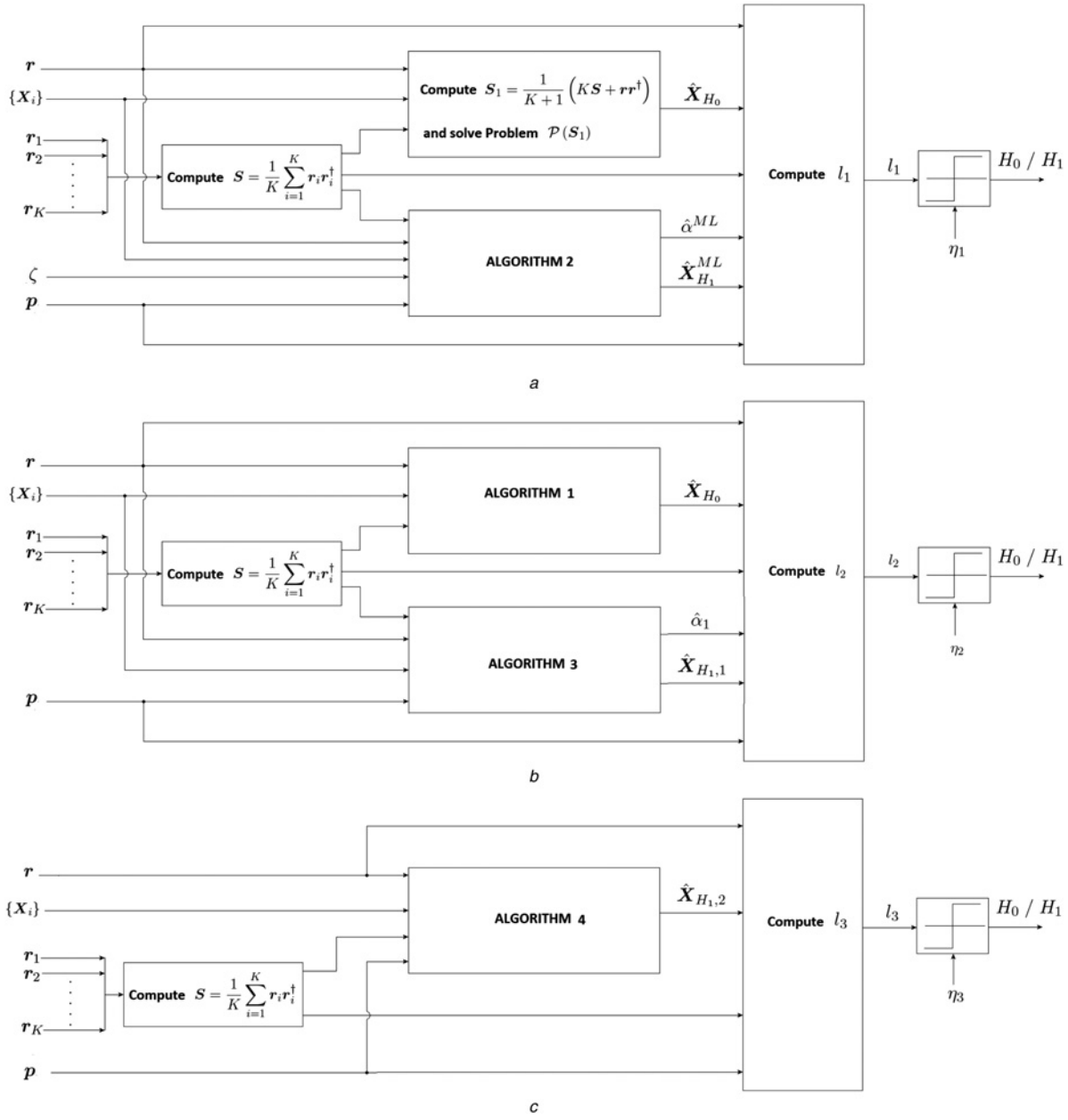

Fig. 5 *Block schemes of the devised GLRT-based detectors*

a GLRT-1 detector
b GLRT-2 detector
c GLRT-3 detector

In *Fig. 5*, the block diagrams of the three new GLRT-based detectors are shown.

4 Performance assessment

In this section, we assess the capability of the proposed covariance matrix estimators to correctly predict the disturbance PSD; besides, we analyse the performance of the devised GLRT-based detectors, in terms of detection probability P_{d}, also in comparison with the optimum detector, which assumes the perfect knowledge of the disturbance covariance matrix, Kelly's GLRT and AMF.

The available multiple a priori models for the interference covariance matrix are assumed Gaussian-shaped [18]; precisely, the (h, k)th entry associated with the ith model, $i = 1, \ldots, H$, is given by

$$\boldsymbol{M}_i(h, k) = \rho_i^{(h-k)^2} \exp\left[j2\pi(h-k)f_i\right] + 10^{-2}\delta_{h,k}$$

where $\delta_{h,k}$ denotes the Kronecker delta function, ρ_i is the one-lag correlation coefficient and f_i represents the normalised Doppler frequency. Moreover, $\boldsymbol{M}_0$ has been set equal to $\boldsymbol{I}$ to account for the receiver noise floor. With this in mind, the inverse interference covariance matrix models are defined as follows:

- $\boldsymbol{X}_0 = \boldsymbol{M}_0^{-1}$;
- $\boldsymbol{X}_i = \boldsymbol{M}_i^{-1}, \quad i = 1, \ldots, H$;

As to the actual covariance matrix, we consider an interference sharing a bimodal PSD accounting for the

doi: 10.1049/iet-rsn.2013.0233

presence of ground and sea clutters in addition to white noise. Assuming an exponentially-shaped PSD for both the interfering sources, the (h, k)th element of the overall normalised disturbance covariance matrix can be expressed as

$$\boldsymbol{M}(h,k) = \mathrm{CNR}_s\ \rho_s^{|h-k|}\exp\left[j2\pi(h-k)f_s\right] + \mathrm{CNR}_g\ \rho_g^{|h-k|}\exp\left[j2\pi(h-k)f_g\right] + \delta_{h,k} \tag{14}$$

where

- $\mathrm{CNR_s}$ and $\mathrm{CNR_g}$ denote, respectively, the clutter-to-noise-ratio (CNR) for the sea and the ground clutter;
- ρ_s and ρ_g are, respectively, the one-lag correlation coefficients for the sea and the ground clutter;
- f_s and f_g, are, respectively, the normalised Doppler frequency for the sea and the ground clutter.

Moreover, we model the target signature $\boldsymbol{p}$ via the conventional Doppler steering vector, that is

$$\boldsymbol{p} = \frac{1}{\sqrt{N}}\left[1, e^{j2\pi f_d}, \ldots, e^{j2\pi f_d(N-1)}\right]^T \tag{15}$$

where f_d is the normalised target Doppler frequency.

It is worth noting that the model used to generate the simulated data does not correspond to any $\boldsymbol{X}_i$, $i = 0, \ldots, H$. In all the simulations, we use the values of the parameters reported in Table 1; additionally, the Doppler frequencies of the a priori models, $\boldsymbol{X}_i$, $i = 1, \ldots, H$, are uniformly distributed over the frequency range $[-(1/2), (1/2)[$, that is

$$f_i = -0.5 + \left(\frac{i-1}{H}\right), \quad i = 1, \ldots, H \tag{16}$$

Finally, to solve the MAXDET problems, we resort to the CVX toolbox [19], a MATLAB package for specifying and solving convex programs.

4.1 PSD analysis

In Figs. 6–8, we plot the actual PSD of the clutter data and its estimates, obtained using the proposed constrained covariance matrix estimators (Algorithms 2–4), for different values of the training data size K and of the a priori model number $H+1$. All the PSDs are computed resorting to the Capon method [20] applied to the appropriate interference covariance matrix, namely the true for the evaluation of the actual PSD and the new estimated covariances for the predicted PSDs.

In each figure and for each algorithm, we show 20 statistically independent PSD realisations as well as their average value. The 20 PSD estimates are drawn from 20 statistically independent snapshots, each composed of $K+1$ independent and identically distributed (i.i.d.) zero mean complex circular Gaussian random vectors sharing the covariance matrix (14). In Fig. 8, for comparison purpose, we also plot the PSD estimated through the sample covariance matrix.

The results show that Algorithms 2 and 4 outperform Algorithm 3. Interestingly, the estimators devised for $H = 20$ ensure better performances than those designed for $H = 5$, highlighting that the models used for $H = 5$ are not able to track the actual interference environment. As a confirmation of such a behaviour, it can be observed that the estimators synthesised for $H = 5$ do not improve their estimation performance as K increases. On the contrary, the estimators, devised for $H = 20$ and based on Algorithms 2 and 4, exhibit better and better performances as the sample support increases; indeed, as K grows up, their capability to correctly match the real clutter PSD shape improves. As a consequence, it can be conjectured that the uncertainty set connected with $H = 20$ well fit the actual operating environment, leading to better and better estimation of the unknown parameters as K increases.

The performed analysis also reveals that, even if a quite reduced sample support ($K = 1$) is available, Algorithm 2 for $H = 20$ is able to suitably track the actual PSD (see Fig. 6). Besides, inspection of Fig. 8 highlights that Algorithms 2 and 4, for $H = 20$, ensure a better estimation performance than the sample covariance matrix. As a final remark, the sample covariance matrix tracks the actual PSD better than Algorithm 3, emphasising the sub-optimality of the last estimator.

Table 1 Parameters used at analysis stage

Parameter	Value
ζ	10^{-2}
N	10
f_d	0.20
f_g	0.05
f_s	0.285
ρ_i	0.90
ρ_g	0.93
ρ_s	0.85
σ^2 [dB]	−10
$\mathrm{CNR_g}$ [dB]	30
$\mathrm{CNR_s}$ [dB]	20

4.2 Detection probability

To evaluate P_d, we set the detection threshold, of each receiver, resorting to Monte-Carlo simulations based on $100/P_{fa}$ independent trials, where P_{fa} represents the desired probability of false alarm; to reduce the computational effort, we set $P_{fa} = 10^{-2}$. The performances are given in terms of P_d against the signal-to-interference plus noise ratio (SINR), defined as

$$\mathrm{SINR} = |\alpha|^2\boldsymbol{p}^\dagger\boldsymbol{M}^{-1}\boldsymbol{p}$$

In the developed analysis, we compare P_d curves of GLRT-1, GLRT-2 and GLRT-3 with those of the benchmark receiver (which assumes the perfect covariance knowledge), Kelly's GLRT and AMF.

In Fig. 9, the results obtained considering $K = 10$ and $H = 14$ are shown. Inspection of the figure highlights that with such a limited amount of secondary data, the AMF and the Kelly's GLRT exhibit unsatisfactory performances, and the proposed adaptive receivers are a viable mean to compensate for the loss experienced by the conventional adaptive structures. Otherwise stated, the new devised detectors are able to guarantee good detection performances even if a small sample support is available. Furthermore, it can be observed that the GLRT-1 and GLRT-3 share almost the same P_d (the curves are nearly overlapped) and exhibit performances very close to the optimum receiver, which

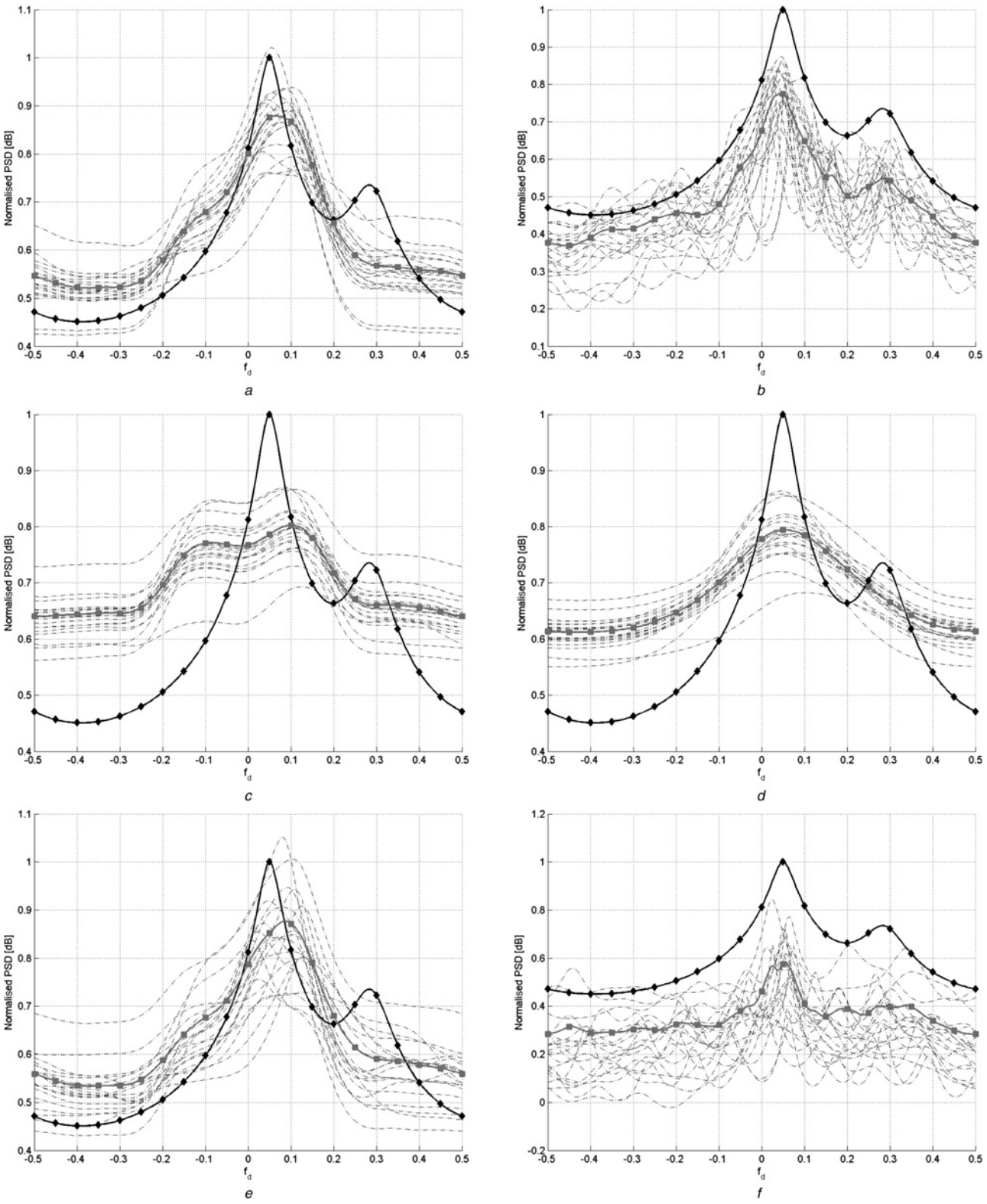

Fig. 6 *Normalised PSD [dB] against normalised Doppler frequency f_d, for the parameters specified in Table 1 and K = 1; in each subplot, the actual PSD (◇-marked curve), 20 PSD realisations for the considered covariance estimator (dashed-dot curves), and their average value (□-marked curve)*

a Algorithm 2, $H = 4$
b Algorithm 2, $H = 20$
c Algorithm 3, $H = 4$
d Algorithm 3, $H = 20$
e Algorithm 4, $H = 4$
f Algorithm 4, $H = 20$

doi: 10.1049/iet-rsn.2013.0233

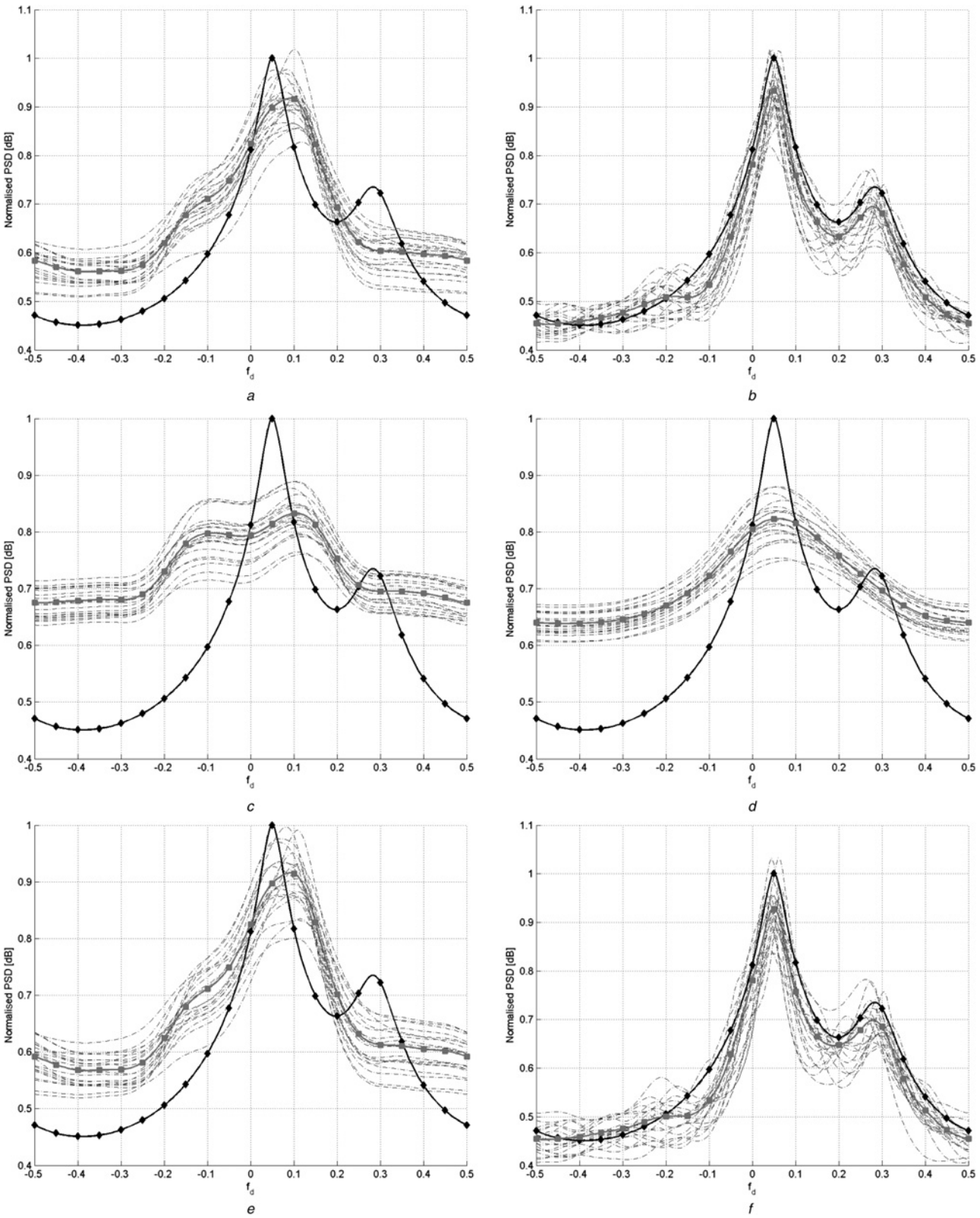

Fig. 7 *Normalised PSD [dB] against normalised Doppler frequency f_d, for the parameters specified in Table 1 and K = 5; in each subplot, the actual PSD (◇-marked curve), 20 PSD realisations for the considered covariance estimator (dashed-dot curves), and their average value (□-marked curve)*

a Algorithm 2, $H = 4$
b Algorithm 2, $H = 20$
c Algorithm 3, $H = 4$
d Algorithm 3, $H = 20$
e Algorithm 4, $H = 4$
f Algorithm 4, $H = 20$

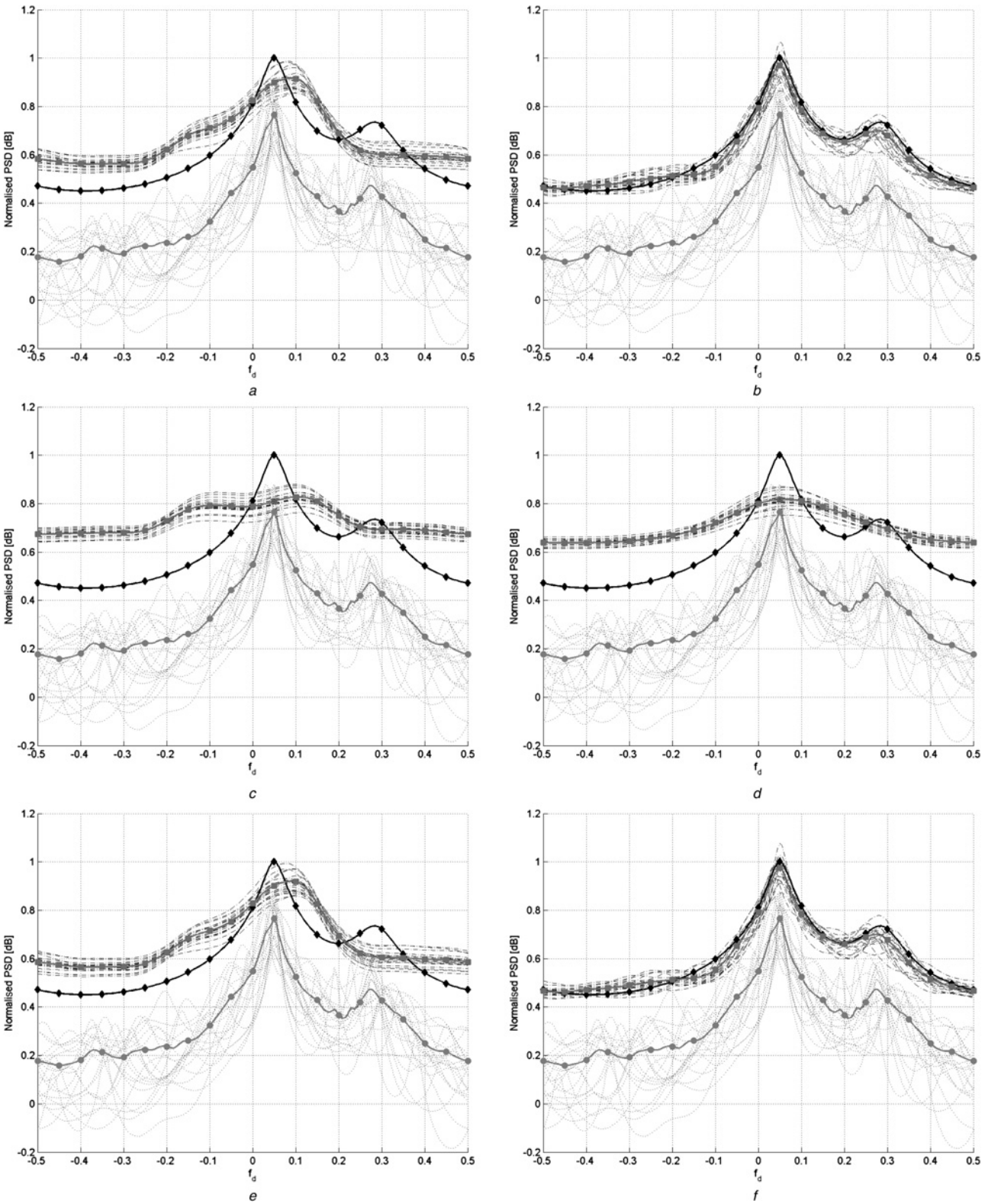

Fig. 8 *Normalised PSD [dB] against normalised Doppler frequency f_d, for the parameters specified in Table 1 and K = 10; in each subplot, the actual PSD (◇-marked curve), 20 PSD realisations for the considered covariance estimator (dashed-dot curves), their average value (□-marked curve), 20 PSD realisations for the sample covariance matrix (dotted curves) and their average value (○-marked curve)*

a Algorithm 2, $H = 4$
b Algorithm 2, $H = 20$
c Algorithm 3, $H = 4$
d Algorithm 3, $H = 20$
e Algorithm 4, $H = 4$
f Algorithm 4, $H = 20$

doi: 10.1049/iet-rsn.2013.0233

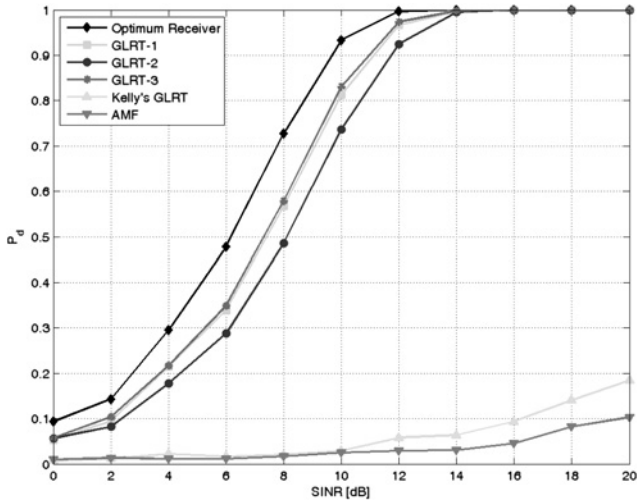

Fig. 9 *P_d against SINR for the parameters specified in Table 1, $K = 10$, and $H = 14$*

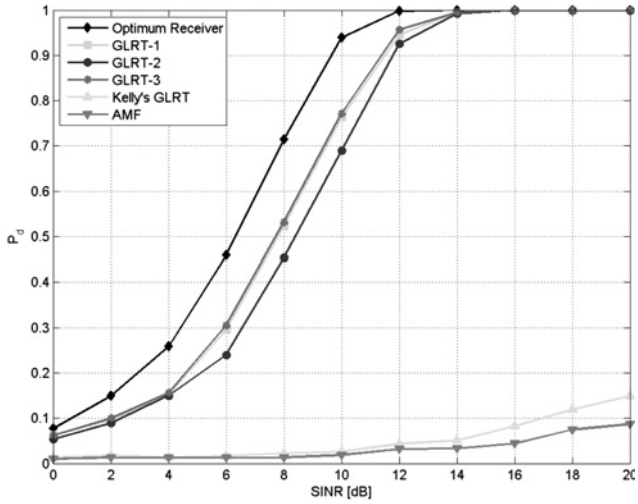

Fig. 10 *P_d against SINR for the parameters specified in Table 1, $K = 10$, and $H = 20$*

assumes the perfect knowledge of the interference covariance matrix. As expected, GLRT-1 and GLRT-3 outperform GLRT-2, which, on the other hand, requires a much lower computational complexity than the counterparts. In Table 2 (the first row) the values of the SINR ensuring $P_d = 0.9$ are shown.

In Fig. 10, to analyse the impact of the adopted model number, the results corresponding to the same scenario as in Fig. 10, but with $H = 20$ are reported. Again, the proposed detectors significantly outperform the conventional ones; moreover, GLRT-1 and GLRT-3 ensure a better performance level than GLRT-2 (see Table 2, second row). Interestingly, the proposed detectors experiment a slight performance degradation as H increases from 14 to 20. We conjecture that, with both $H = 14$ and $H = 20$, the assumed uncertainty set well fit the actual covariance matrix, so as with $H = 14$ better performances can be achieved (a reduced number of parameters has to be estimated).

Finally, in Fig. 11, P_d curves are shown assuming the same scenario as in Fig. 10 but $K = 20$. The receivers can take advantage of the higher number of training data. Specifically, the performances of the AMF and Kelly's GLRT significantly improve with respect to the case $K = 10$, but they are still outperformed by the proposed adaptive detectors. As in Fig. 10, GLRT-1 and GLRT-3 ensure almost the same performances and achieve a better detection probability than GLRT-2. Finally, the three proposed adaptive receivers are closer to the optimum receiver than in the case $K = 10$. This is not surprising, since higher number of secondary data allows to better estimate the unknown parameters. In Table 2 (the third row), the list of the SINR values required to obtain $P_d = 0.9$ is shown. In summary, the performed analysis highlights that the proposed adaptive receivers, based on a smart use of multiple a priori models, exhibit better detection

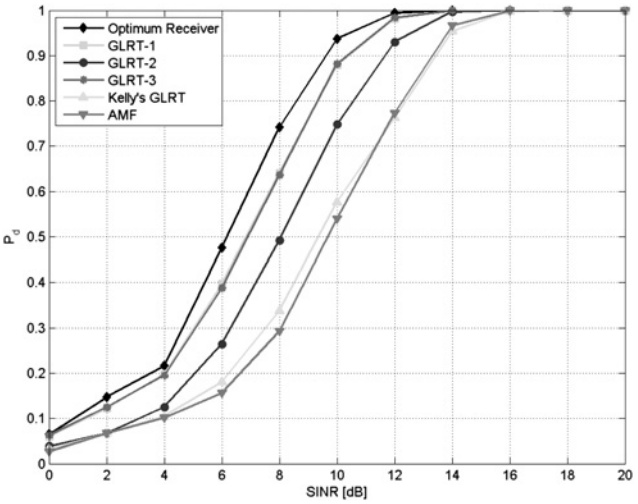

Fig. 11 *P_d against SINR for the parameters specified in Table 1, $K = 20$, and $H = 20$*

performances than the conventional adaptive receivers, especially in environments with a limited number of homogeneous secondary data.

5 Conclusions

In this paper we have considered the problem of adaptive radar detection in operating environments characterised by a limited number of training data. We have proposed three GLRT-based detection schemes assuming that the inverse

Table 2 SINR values in dB required to achieve $P_d = 0.9$

	GLRT-1	GLRT-2	GLRT-3	Optimum receiver	AMF	Kelly's GLRT
$K = 10$, $H = 14$	10.90	11.72	11.12	9.68	—	—
$K = 10$, $H = 20$	11.38	11.78	11.50	9.68	—	—
$K = 20$, $H = 20$	10.39	11.65	10.39	9.60	13.31	13.41

covariance matrix is modelled as a linear combination of some available a priori models and accounting for the knowledge of a lower bound on the PSD of the white disturbance term. The computational complexity of the proposed adaptive receivers is different; specifically, GLRT-1 is more demanding, since it involves an iterative procedure, where in each step the optimum values of a convex optimisation MAXDET problem is required; GLRT-3 does not require iterative optimisations but the optimal solution of just one MAXDET problem. Finally, GLRT-2 is less demanding since it does not require iterative optimisations and the solution for MAXDET problems.

At the analysis stage, we have analysed the capability of the proposed covariance matrix estimators, involved in the devised detectors, to predict the actual interference environment. The results have highlighted that the new techniques (especially those connected with GLRT-1 and GLRT-3) are able to track the actual PSD of the data from the cell under test. Besides, we have assessed the performance of the new adaptive receivers in terms of detection probability, in comparison with the optimum benchmark receiver (which assumes the perfect knowledge of the disturbance covariance matrix) and two conventional adaptive detectors Kelly's GLRT and AMF. The results have shown that in the presence of a small number of training data the new receiving structures exhibit an acceptable performance loss with respect to the benchmark and a significant performance gain over the conventional adaptive counterparts.

A possible future research track might concern the performance analysis of the proposed detectors on real radar data as well as the exploitation, at the design stage, of both a structural constraint and a condition number constraint [21], to further improve the covariance matrix estimation process.

6 References

1 Reed, I.S., Mallett, J.D., Brennan, L.E.: 'Rapid convergence rate in adaptive arrays', *IEEE Trans. Aerosp. Electron. Syst.*, 1974, **10**, (4), pp. 853–863

2 Kelly, E.J.: 'An adaptive detection algorithm', *IEEE Trans. Aerosp. Electron. Syst.*, 1986, **22**, (1), pp. 115–127

3 Robey, F.C., Fuhrmann, D.R., Kelly, E.J., Nitzberg, R.: 'A CFAR adaptive matched filter detector', *IEEE Trans. Aerosp. Electron. Syst.*, 1992, **28**, (1), pp. 208–216

4 Richmond, C.D.: 'Performance of a class of adaptive detection algorithms in nonhomogeneous environments', *IEEE Trans. Signal Process.*, 2000, **48**, (5), pp. 1248–1262

5 Melvin, W.L.: 'Space-time adaptive radar performance in heterogeneous clutter', *IEEE Trans. Aerosp. Electron. Syst.*, 2000, **36**, (2), pp. 621–633

6 Gini, F. (ed.): 'Knowledge-based systems for adaptive radar: detection, tracking, and classification', *IEEE Signal Process. Mag.*, 2006, **23**, (1), pp. 14–76

7 Guerci, J.R., Melvin, W.L. (ed.): 'Special section on knowledge-aided sensor signal and data processing', *IEEE Trans. Aerosp. Electron. Syst.*, 2006, **42**, (3), pp. 983–1120

8 Hao, C., Orlando, D., Ma, X., Hou, C.: 'Persymmetric Rao and Wald tests for partially homogeneous environment', *IEEE Signal Process. Lett.*, 2012, **19**, (9), pp. 587–590

9 Aubry, A., De Maio, A., Pallotta, L., Farina, A.: 'Radar detection of distributed targets in homogeneous interference whose inverse covariance structure is defined via unitary invariant functions', *IEEE Trans. Signal Process.*, **61**, (20), pp. 4949–4961

10 Steiner, M., Gerlach, K.: 'Fast converging adaptive processors or a structured covariance matrix', *IEEE Trans. Aerosp. Electron. Syst.*, 2000, **36**, (4), pp. 1115–1126

11 Aubry, A., De Maio, A., Carotenuto, V.: 'Optimality claims for the FML covariance estimator with respect to two matrix norms', *IEEE Trans. Aerosp. Electron. Syst.*, in press

12 Vandenberghe, L., Boyd, S., Wu, S.P.: 'Determinant maximization with linear matrix inequality constraints', *SIAM J. Matrix Anal. Appl.*, 1998, **19**, pp. 499–533

13 De Maio, A., Foglia, G., Farina, A., Piezzo, M.: 'Estimation of the covariance matrix based on multiple a priori models'. IEEE Radar Conference, Washington DC, USA, 10–14 May 2010, pp. 1025–1029

14 Aubry, A., De Maio, A., Pallotta, L., Farina, A.: 'Covariance matrix estimation via geometric barycenters and its application to radar training data selection', *IET Radar Sonar Navig.*, 2013, **7**, (6), pp. 600–614

15 Chen, P., Melvin, W.L., Wicks, M.C.: 'Screening among multivariate normal data', *J. Multivariate Anal.*, 1999, **69**, (1), pp. 10–29

16 Himed, B., Melvin, W.L.: 'Analyzing space-time adaptive processors using measured data'. Proc. 31st Asilomar Conf. Signals, Systems & Computers, Pacific Grove (CA), USA, November 1997, pp. 930–935

17 Nemirovski, A.: 'Lectures on Modern Convex Optimization'. Available at: http://www.isye.gatech.edu/faculty-staff/profile.php?entry=an63

18 Farina, A., Gini, F., Greco, M.V., Lee, P.H.Y.: 'Improvement factor for real sea-clutter Doppler frequency spectra', *IET Proc. Radar Sonar Navig.*, 1996, **143**, (5), pp. 341–344

19 CVX Research, Inc. CVX: Matlab Software for Disciplined Convex Programming, version 2.0 beta. http://cvxr.com/cvx, September 2012

20 Stoica, P., Moses, R.: 'Introduction to spectral analysis' (Prentice-Hall, NJ, 1997)

21 Aubry, A., De Maio, A., Pallotta, L., Farina, A.: 'Maximum likelihood estimation of a structured covariance matrix with a condition number constraint', *IEEE Trans. Signal Process.*, 2012, **60**, (6), pp. 3004–3021

7 Appendix

7.1 Appendix 1: Proof of Proposition 1

Proof: Let us show that problem $\mathcal{P}(\boldsymbol{S}_1)$ is solvable for any $\boldsymbol{S}_1 \succeq \boldsymbol{0}$. To this end, we notice that

$$\mathrm{tr}\{\boldsymbol{S}\boldsymbol{X}\} - \log\,\det(\boldsymbol{X}) \geq -\log\left(\lambda_{\min}(\boldsymbol{X})\right) + (N-1)\log\left(\sigma^2\right) \tag{17}$$

where the inequality stems from $\mathrm{tr}\{\boldsymbol{S}\boldsymbol{X}\} \geq 0$ and $(1/\sigma^2) \geq \lambda_1(\boldsymbol{X}) \geq \cdots \geq \lambda_N(\boldsymbol{X}) = \lambda_{\min}(\boldsymbol{X})$, with $\lambda_i(\boldsymbol{X})$, $i = 1, \ldots, N$ the eigenvalues of $\boldsymbol{X}$. Hence, when $\boldsymbol{X}$ tends to a rank deficient matrix, the objective function tends to $+\infty$. As a consequence, there exists $\epsilon > 0$ such that $\mathcal{P}(\boldsymbol{S}_1)$ is equivalent to

$$\mathcal{P}' \begin{cases} \min\limits_{\boldsymbol{X}} & \mathrm{tr}(\boldsymbol{S}_1\boldsymbol{X}) - \log\,\det(\boldsymbol{X}) \\ \text{subject to} & \boldsymbol{X} \in \mathcal{A} \\ & \boldsymbol{X} \succeq \epsilon\boldsymbol{I} \end{cases} \tag{18}$$

Notice that the objective function of problem $\mathcal{P}'$ is a continuous function and the constraint set defines a compact set. Indeed, the feasible set of $\mathcal{P}'$ is the intersection between the compact set $\epsilon\boldsymbol{I} \preceq \boldsymbol{X}(1/\sigma^2)\boldsymbol{I}$ and a linear subspace of finite dimension. Thus, Weierstrass theorem ensures the existence of a feasible point $\boldsymbol{X}^\star$ for $\mathcal{P}'$ such that $v(\mathcal{P}') = \mathrm{tr}\{\boldsymbol{S}\boldsymbol{X}^\star\} - \log\,\det(\boldsymbol{X}^\star)$. Finally, let us observe that the objective function of problem $\mathcal{P}(\boldsymbol{S}_1)$ is strictly convex, and the constraint (4) defines a convex set. Hence, the optimal solution to $\mathcal{P}(\boldsymbol{S}_1)$ is unique.

7.2 Appendix 2: Proof of Proposition 2

Proof: We first prove that $\mathrm{ML}^{(n)}$ is a monotone increasing sequence, that is, $\mathrm{ML}^{(n)} \leq \mathrm{ML}^{(n+1)}$. In fact, we have

$$\mathrm{ML}^{(n)} = \frac{\det\left(\hat{\boldsymbol{X}}_{H_1}^{(n)}\right)^{K+1}}{\pi^{N(K+1)}} \exp\left(-\mathrm{tr}\left\{\hat{\boldsymbol{X}}_{H_1}^{(n)}\left(\boldsymbol{R}_{\hat{\alpha}^{(n)}} + K\boldsymbol{S}\right)\right\}\right) \tag{19}$$

doi: 10.1049/iet-rsn.2013.0233

$$\leq \frac{\det\left(\hat{\boldsymbol{X}}_{H_1}^{(n+1)}\right)^{K+1}}{\pi^{N(K+1)}} \exp\left(-\mathrm{tr}\left\{\hat{\boldsymbol{X}}_{H_1}^{(n+1)}\left(\boldsymbol{R}_{\hat{\alpha}^{(n)}} + K\boldsymbol{S}\right)\right\}\right) \quad (20)$$

$$\leq \frac{\det\left(\hat{\boldsymbol{X}}_{H_1}^{(n+1)}\right)^{K+1}}{\pi^{N(K+1)}} \exp\left(-\mathrm{tr}\left\{\hat{\boldsymbol{X}}_{H_1}^{(n+1)}\left(\boldsymbol{R}_{\hat{\alpha}^{(n+1)}} + K\boldsymbol{S}\right)\right\}\right)$$
$$= \mathrm{ML}^{(n+1)} \quad (21)$$

As to the convergence of the sequence $\mathrm{ML}^{(n)}$, let us observe that, for all $\hat{\alpha}$ and $\hat{\boldsymbol{X}}$

$$\frac{\det(\hat{\boldsymbol{X}})^{K+1}}{\pi^{N(K+1)}} \exp\left(-\mathrm{tr}\left\{\hat{\boldsymbol{X}}\left(\boldsymbol{R}_{\hat{\alpha}} + K\boldsymbol{S}\right)\right\}\right)$$
$$\leq \frac{\det(\hat{\boldsymbol{X}})^{K+1}}{\pi^{N(K+1)}} \exp\left(-\mathrm{tr}\left\{\hat{\boldsymbol{X}}(K\boldsymbol{S})\right\}\right) \quad (22)$$

$$\leq \frac{\det(\hat{\boldsymbol{X}}_0)^{K+1}}{\pi^{N(K+1)}} \exp\left(-\mathrm{tr}\left\{\hat{\boldsymbol{X}}_0(K\boldsymbol{S})\right\}\right) \quad (23)$$

with $\hat{\boldsymbol{X}}_0$ the optimal solution to problem $\mathcal{P}(\boldsymbol{S}_1)$, with $\boldsymbol{S}_1 = \dfrac{K\boldsymbol{S}}{(K+1)}$, whose existence is ensured by Proposition 1. Hence, $\mathrm{ML}^{(n)}$ converges to a finite value $\mathrm{ML}^{\star}$, since it is an upper bounded monotonic increasing sequence.